

# Probing helium reionization with kinetic Sunyaev-Zel'dovich tomography

Selim C. Hotinli<sup>1</sup>, Simone Ferraro<sup>2,3</sup>, Gilbert P. Holder<sup>4,5</sup>, Matthew C. Johnson<sup>6,7</sup>,  
Marc Kamionkowski<sup>1</sup>, and Paul La Plante<sup>3,8,9</sup>

<sup>1</sup>*William H. Miller III Department of Physics and Astronomy, Johns Hopkins University,  
Baltimore, Maryland 21218, USA*

<sup>2</sup>*Lawrence Berkeley National Laboratory, One Cyclotron Road, Berkeley, California 94720, USA*

<sup>3</sup>*Berkeley Center for Cosmological Physics, Department of Physics, University of California,  
Berkeley, California 94720, USA*

<sup>4</sup>*Astronomy Department, University of Illinois at Urbana-Champaign,  
1002 West Green Street, Urbana, Illinois 61801, USA*

<sup>5</sup>*Department of Physics, University of Illinois Urbana-Champaign,  
1110 West Green Street, Urbana, Illinois 61801, USA*

<sup>6</sup>*Perimeter Institute for Theoretical Physics, 31 Caroline Street North,  
Waterloo, Ontario N2L 2Y5, Canada*

<sup>7</sup>*Department of Physics and Astronomy, York University, Toronto, Ontario M3J 1P3, Canada*

<sup>8</sup>*Department of Computer Science, University of Nevada, Las Vegas, Nevada 89154, USA*

<sup>9</sup>*Nevada Center for Astrophysics, University of Nevada, Las Vegas, Nevada 89154, USA*



(Received 23 July 2022; revised 6 October 2022; accepted 12 April 2023; published 15 May 2023)

Reionization of helium is expected to occur at redshifts  $z \sim 3$  and have important consequences for quasar populations, galaxy formation, and the morphology of the intergalactic medium, but there is little known empirically about the process. Here we show that kinetic Sunyaev-Zel'dovich tomography, based on the combination of cosmic microwave background (CMB) measurements and galaxy surveys, can be used to infer the primordial helium abundance as well as the time and duration of helium reionization. We find a high-significance detection at  $\sim 10\sigma$  can be expected from Vera Rubin Observatory and CMB-S4 in the near future. A more robust characterization of helium reionization will require next-generation experiments like MegaMapper (a proposed successor to the Dark Energy Spectroscopic Instrument) and CMB-HD.

DOI: [10.1103/PhysRevD.107.103517](https://doi.org/10.1103/PhysRevD.107.103517)

Probing helium reionization<sup>1</sup>—one of the major large-scale transitions of the intergalactic medium (IGM)—has great potential significance for understanding the formation of galaxies and quasar activity at early times and may open a new window on big bang nucleosynthesis. Since photons emitted by the first stars (sourcing the reionization of hydrogen) are not energetic enough<sup>2</sup> to fully ionize helium, helium reionization occurs only after the emergence of a substantial number of quasars. As a result, the history of helium reionization strongly depends on the properties of quasars, such as their luminosity function [1–5], accretion mechanisms and other astrophysics [6], clustering, variability, and lifetimes [7,8], as well as the general growth and evolution of supermassive black holes [9]. Since essentially all of the helium in the Universe is ultimately doubly ionized, the total change in the ionization fraction is a measure of the primordial helium abundance—a sensitive

probe of big bang nucleosynthesis. Probing helium reionization can also improve our understanding of relativistic species through improving the primordial helium fraction  $Y_p$  measurement and breaking the degeneracy between number of relativistic degrees of freedom  $N_{\text{eff}}$  and  $Y_p$ . The primordial helium abundance depends on the weak interaction rates as well as the neutron lifetime, and improving its measurement can allow further valuable insights into our cosmological history.

There is evidence for quasar activity peaking around  $z \sim 3$  [10], which coincides with measurements of the helium Ly $\alpha$  forest, suggesting the helium in the IGM has not yet been doubly ionized [11–13]. Measurements of the thermal history of the IGM have provided indirect evidence for helium reionization occurring roughly  $2.5 \lesssim z \lesssim 4$  [14–16], with seminumeric and hydrodynamic simulations of helium reionization supporting a similar picture [17–20]. Nevertheless, the precise details of the timing, duration, and morphology of helium reionization remain largely uncertain. Surveys of the helium Ly $\alpha$  forest are severely limited by intervening Lyman-limit systems at lower redshift [21], which means it will be challenging to

<sup>1</sup>Note that throughout this work we refer to the ionization of the second electron of helium as the helium reionization.

<sup>2</sup>The ionization energy of the second electron in helium is 54.4 eV, while the ionization energy of hydrogen is 13.6 eV.

make further progress. Furthermore, measurements of the hydrogen Ly $\alpha$  forest can probe the thermal history of the IGM, which provides indirect evidence for details of helium reionization that result from photoheating. However, such measurements are difficult in practice and are subject to systematic uncertainties about the inferred flux levels of the Ly $\alpha$  forest and modeling fits to the thermal equation of state of the IGM [22–24]. Additional probes of helium reionization will be incredibly valuable. For example, it has been shown that future large catalogs of fast radio bursts could probe helium reionization [25,26].

In this paper, we propose a new way to detect and characterize helium reionization by means of tomography using the kinetic Sunyaev-Zel’dovich (KSZ) effect [27]. This KSZ tomography has been shown to be an effective way to extract cosmological information (through the reconstructed radial-velocity field) from small-scale fluctuations in the cosmic microwave background (CMB) and a tracer of the electron density, such as a galaxy survey (e.g. [28–37]). Ongoing large-scale structure surveys that access  $2 < z < 5$  galaxy and quasar populations such as the Dark Energy Spectroscopic Instrument (DESI) [38] or the Rubin Observatory Legacy Survey of Space and Time (LSST) [39] are opening a new window of opportunity into probing the Universe at largely uncharted epochs of structure formation. Cross-correlation of large-scale structure (LSS) measured at these redshifts with maps of the CMB can be a powerful probe in the near future. We demonstrate that, by measuring the statistical variations of the cross-correlation between the LSS and CMB, one can probe the change in the mean ionization fraction during the epoch of helium reionization to high significance with upcoming surveys such as CMB-S4 [40,41], together with DESI, LSST or the proposed MegaMapper [42,43].

The summary of our procedure is as follows: we get the galaxy density field from large-scale structure surveys. We use this galaxy density field on *small scales* to template the electron distribution, which we use in cross-correlation with the CMB signal to isolate the KSZ signal and reconstruct the large-scale radial velocity fluctuations that the KSZ signal is subject to (this procedure is called “KSZ tomography”). We then compare the auto- and cross-spectra of the velocity reconstructed using KSZ tomography and the galaxy density field from large-scale structure surveys on *large scales* to measure  $x_e$  in several redshift bins (of width  $L_{\text{shell}}$ ).

The CMB temperature anisotropy induced by the KSZ effect from large-scale structure in a shell of width  $L_{\text{shell}}$  at a redshift  $z = z_*$  is

$$\Theta_{\text{KSZ}}(\boldsymbol{\theta}) = K(z_*) \int_{-L_{\text{shell}}/2}^{L_{\text{shell}}/2} d\mathbf{r} q_{\parallel}(\mathbf{r}), \quad (1)$$

where  $q_{\parallel}(\mathbf{r}) = \delta_e(\mathbf{r})v_{\parallel}(\mathbf{r})$  is the electron-momentum field, projected onto the radial direction,  $\mathbf{r} \equiv \chi_* \boldsymbol{\theta} + r\hat{\mathbf{r}}$ ,  $\boldsymbol{\theta}$  is the angular direction on the sky,  $\chi_*$  is the conformal distance to the shell,  $\hat{\mathbf{r}}$  is the unit vector in the radial direction,  $\Theta(\boldsymbol{\theta})$  is the fractional fluctuation of CMB temperature, and

$$K(z) = -\sigma_T n_{\text{H}} x_e(z) e^{-\tau(z)} (1+z)^2 \quad (2)$$

is the radial weight function in units of  $\text{Mpc}^{-1}$ . Here,  $\sigma_T$  is the Thomson scattering cross section,  $\tau(z)$  is the optical depth to redshift  $z$ ,  $n_{\text{H}}$  is the hydrogen number density, and  $x_e(z)$  is the number of free electrons per hydrogen atom. The velocity field  $v_{\parallel}(\mathbf{r})$  can be reconstructed at cosmological scales from its influence on the correlation between the electron-momentum field and large-scale structure, as shown with derivations for the box formalism we employ in Sec. IV E of Ref. [29] and previously for the full sky in Sec. II B of Ref. [28]. The (inverse) noise on the reconstructed velocity is given by [28–30]

$$\frac{1}{N_{\parallel}(\mathbf{k}_L)} = \frac{K_*^2}{\chi_*^2} \int \frac{k_s dk_s}{2\pi} \left( \frac{P_{\text{ge}}(k_s)^2}{P_{\text{gg}}^{\text{obs}}(k_s) C_{\ell}^{\text{TT,obs}}} \right)_{\ell=k\chi_*}, \quad (3)$$

where  $K_* \equiv K(z_*)$ ,  $\mathbf{k}$  is the three-dimensional Fourier wave vector and the integral is over small-scale Fourier modes  $k_s$ . We represent large-scale modes with an “L” subscript. Here,  $C_{\ell}^{\text{TT,obs}}$  is the observed CMB spectrum including foregrounds and noise,  $P_{\text{gg}}^{\text{obs}}(k)$  is the observed galaxy power spectrum and  $P_{\text{ge}}(k)$  is the power spectrum of the galaxy-electron correlation.

On large scales where linear theory is valid, the reconstructed velocity fields are proportional to the cosmic growth rate. The reconstructed velocity amplitude is proportional to the free-electron density at a given redshift and satisfies

$$\hat{v}_{\parallel}(\mathbf{k}, z) = [\bar{x}_e(z)/\bar{x}_e(z)_{\text{fid}}] b_{\parallel}(z) \mu \frac{faH}{k} \delta_{\text{m}}(z, \mathbf{k}), \quad (4)$$

where  $\bar{x}_e(z)/\bar{x}_e(z)_{\text{fid}}$  is equal to unity for a given fiducial cosmology with helium reionization,  $b_{\parallel}(z)$  is the optical-depth bias due to mismodeling of the small-scale electron-galaxy cross-correlation as described in Refs. [28–30],  $f \equiv d \ln D(a)/d \ln a$  is the linear-theory growth rate, where  $D(a)$  is the linear-theory growth factor for the matter spectrum that parametrizes the time evolution of the matter power spectra via  $P_{\text{mm}}(a) = D^2(a)P_{\text{mm}}(a=1)$ ,  $a$  is the scale factor and  $H$  is the Hubble parameter. As a result, the reconstructed velocity fields probe the mean ionization fraction: if the helium reionization is not accounted for, the velocity amplitudes will be biased by the change of the mean reionization fraction. The combination of the galaxy and the velocity satisfies

$$P_{gg}(k, \mu, z) = (b_g(z) + f\mu^2)^2 P_{mm}(k, z), \quad (5)$$

$$P_{vv}(k, \mu, z) = \left( \frac{\bar{x}_e(z)}{\bar{x}_e(z)_{\text{fid}}} \right)^2 b_{\parallel}(z)^2 \left( \frac{faH}{k} \right)^2 P_{mm}(k, z), \quad (6)$$

$$P_{gv}(k, \mu, z) = \left( \frac{\bar{x}_e(z)}{\bar{x}_e(z)_{\text{fid}}} \right) b_{\parallel}(z) \left( \frac{faH}{k} \right) \times (b_g(z) + f\mu^2) P_{mm}(k, z), \quad (7)$$

where  $b_g(z)$  is the galaxy bias which relates the matter distribution to the galaxy.

We characterize the change in the ionization fraction during helium reionization with a hyperbolic tangent

$$\bar{x}_e(z) = \frac{1}{2} \left[ 2 + \Delta\bar{x}_{\text{He}} + \Delta\bar{x}_{\text{He}} \tanh\left(\frac{y(z_{\text{re}}^{\text{He}}) - y(z)}{\Delta_y^{\text{He}}}\right) \right], \quad (8)$$

as commonly done in the standard theory codes such as CAMB [44]. Here,  $y(z) = (1+z)^{3/2}$ ,  $\Delta\bar{x}_{\text{He}}$  determines the total change in the mean ionization fraction during helium reionization,  $z_{\text{re}}^{\text{He}}$  is the redshift halfway through the helium reionization and  $\Delta_y^{\text{He}}$  parametrizes the duration of the transition. In what follows we will trade  $\Delta\bar{x}_{\text{He}}$  with  $Y_p$  and use CAMB to calculate  $\partial Y_p / \partial \Delta\bar{x}_{\text{He}}$  and the  $\Delta_y^{\text{He}}$  parameter with  $\Delta_z^{\text{He}}$ , which we define as the duration in redshift of the central 50% change in ionization fraction. In Fig. 1, we demonstrate three reionization models labeled with numbers 1–3 with fiducial choices for  $(z_{\text{re}}^{\text{He}}, \Delta_z^{\text{He}})$  set equal to (3.34, 0.8), (2.29, 0.79) and (4.14, 0.58), respectively. We take  $Y_p = 0.245$  for all models. These models are chosen

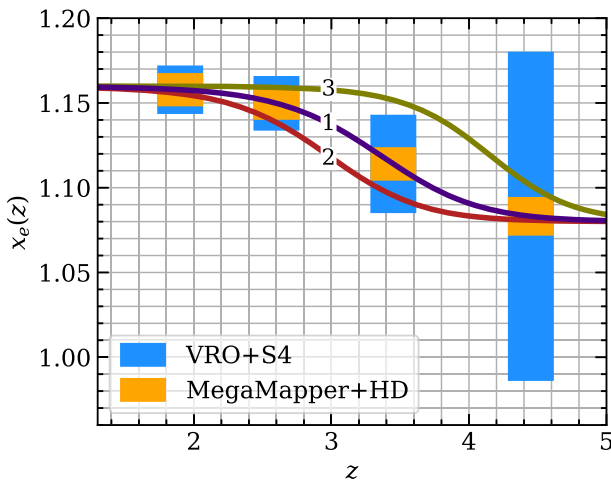


FIG. 1. Fractional change in the electron fraction  $x_e(z)$  during helium reionization of the three models we consider here. The error bars correspond to the measurement accuracy on the optical-depth bias  $b_{\parallel}(z)$ , representative of the error on the amplitude of the reconstructed radial velocity, as discussed in the text. Here, we include forecasts for the combination of LSST and CMB-S4, and MegaMapper and CMB-HD [49].

to roughly match models H1, H3 and H6, considered in Ref. [45], respectively, and represent several plausible models of helium reionization. Model H1 reproduces the quasar abundance measured by Refs. [1–3], the typical quasar spectrum measured by Ref. [46], and quasar clustering measured by BOSS [47]. Model H3 uses a quasar abundance reduced by a factor of 2, which is consistent with the measured uncertainties but yields a slightly later reionization scenario. Model H6 uses a uniform UV background rather than explicit quasar sources and reproduces the seminumeric models of Ref. [48]. Distinguishing between these models can provide an independent determination of the average abundance and luminosity of quasars, which complements direct measurements from surveys like the Sloan Digital Sky Survey. Quasar activity also significantly heats the IGM, which in turn affects measurements of the low-density gas in the Ly $\alpha$  forest.

In order to assess the prospects to detect helium reionization, we consider three LSS surveys: the ongoing measurements of quasistellar objects with DESI [38], the photometric LSST survey [39], and high- $z$  galaxy measurements from the proposed MegaMapper [42]. We describe the survey specification of these experiments in Table I.<sup>3</sup> We consider four redshift boxes centered at  $z \in \{1.9, 2.6, 3.45, 4.45\}$ . We assume a sky fraction of  $f_{\text{sky}} \simeq 0.5$  which roughly gives volumes of  $\{150, 200, 220, 240\}$  Gpc<sup>3</sup> at each redshift box, respectively.<sup>4</sup>

The total CMB power gets contributions from weak gravitational lensing, the KSZ effect (both from reionization and late times), and other foregrounds, as well as experimental noise satisfying

$$N_{\ell} = \Delta_T^2 \exp \left[ \frac{\ell(\ell+1)\theta_{\text{FWHM}}^2}{8 \ln 2} \right], \quad (9)$$

where we consider three CMB experiments with white noise specifications matching Simons Observatory (SO) [53], CMB-S4 [40] and CMB-HD [49] as given in Table II. We also include the frequency-dependent clustered cosmic infrared background (CIB), Poisson CIB and thermal Sunyaev Zeldovich effect (tSZ) foregrounds, the blackbody late-time

<sup>3</sup>A quick forecast of DESI quasars, calculating the number density following Ref. [38] and setting the bias to satisfy  $b_g(z) = 1.2/D(z)$ , shows that it would be difficult to detect helium reionization with these data due to low number density of quasars anticipated to be observed at high redshifts. We drop DESI from our analysis in what follows.

<sup>4</sup>Note that our forecast in this work ignores the time evolution of power spectra and biases on the light cone inside individual redshift boxes but is sensitive to the light-cone evolution by using a sequence of boxes of the appropriate volume for a series of redshift bins along the light cone. Throughout we take the standard six-parameter  $\Lambda$ CDM model, in which the universe is composed of dark energy, cold dark matter and ordinary matter, with fiducial values from Planck [50] and assume reionization of hydrogen and the first electron in helium was completed by  $z \simeq 5$ .

TABLE I. Assumed galaxy bias  $b_g$  and number density  $n_{\text{gal}}$  at each redshift bin. For LSST, we approximate the galaxy density of the “gold” sample, with  $n(z) = n_{\text{gal}}[(z/z_0)^2 \exp(-z/z_0)/2z_0]$  with  $n_{\text{gal}} = 40^{-2}$  and  $z_0 = 0.3$ , and take the galaxy bias as  $b_g(z) = 0.95/D(z)$ . Our calculation of the number density and the galaxy bias of MegaMapper, which is proposed as a follow-up to DESI that will target Lyman-break galaxies and Lyman-alpha emitters and use deeper LSST images, is described in Ref. [51], which follows Ref. [38], using galaxies with threshold apparent magnitude  $m_V^{\text{th}} = 24.5$  (matching the limiting magnitude assumed for the “idealized sample” from Ref. [38]) and using the “linear halo occupation distribution (HOD) model” fit of Ref. [52] at  $z \simeq 3.8$ . For LSST, we consider the standard anticipated photo- $z$  error  $\sigma_z = 0.03(1+z)$  which becomes increasingly more detrimental at higher redshifts. The Y1 and Y10 correspond to our assumed galaxy number densities for LSST after the first and tenth year of observations, respectively.

	$z = 1.9$	2.6	3.45	4.45	
LSST					
$b_g$	1.81	2.47	3.28	4.23	
$n_{\text{gal}} (\times 10^4) [\text{Mpc}^{-3}]$	5.8	1.2	0.13	0.01	Y1
$n_{\text{gal}} (\times 10^4) [\text{Mpc}^{-3}]$	14.9	2.9	0.34	0.02	Y10
MegaMapper					
$b_g$	1.92	3.18	4.71	6.51	
$n_{\text{gal}} (\times 10^4) [\text{Mpc}^{-3}]$	11.7	3.4	1	0.2	

and reionization KSZ, and radio sources as described in Ref. [54].

We calculate the lensed CMB blackbody using CAMB [55]. Our internal linear combination method (ILC)-cleaning procedure is explained in Ref. [54].<sup>5</sup>

In addition to the three parameters defined above that characterize the helium reionization, we model the galaxy and velocity power spectra with the linear-theory growth rate  $f$ , the amplitude  $\sigma_8$  of matter fluctuations on the scale of  $8h^{-1}$  Mpc, and independent galaxy and optical-depth bias parameters  $b_g(z)$  and  $b_{\parallel}(z)$  at each redshift.<sup>6</sup> Note that, throughout this work, we assume measurements at lower redshifts will provide  $\lesssim 1\%$  priors on  $f$  and  $\sigma_8$ , although our results for helium reionization parameters do not significantly depend on this prior.

Figure 1 demonstrates the measurement accuracy of the radial-velocity amplitude for combinations of LSST and MegaMapper surveys with CMB-S4 and CMB-HD, respectively. The signal-to-noise (SNR) of the KSZ tomography at each redshift is shown in Table III for a wider selection of CMB and LSS experimental configurations. Here, we define the detection SNR of helium reionization as the SNR on

<sup>5</sup>Foregrounds such as tSZ, CIB or CMB lensing are found to not be a significant source of bias for velocity tomography in Ref. [56] since most non-KSZ secondaries are even under radial reflection symmetry, whereas the KSZ is odd.

<sup>6</sup>The vector of parameters we consider in this analysis is  $\vec{p} = \{f, \sigma_8, b_g(z_1), \dots, b_g(z_4), b_{\parallel}(z_1), \dots, b_{\parallel}(z_4), z_{\text{re}}^{\text{He}}, \Delta_z^{\text{He}}, Y_p\}$ , where  $z_1, \dots, z_4$  correspond to the four redshift bins we consider.

TABLE II. Inputs to ILC noise: the beam and noise rms parameters we assume for survey configurations roughly corresponding to SO (baseline), CMB-S4 and CMB-HD [49].

	Beam FWHM			Noise rms $\mu\text{K}'$		
	SO	CMB-S4	CMB-HD	SO	CMB-S4	CMB-HD
39 GHz	5.1'	5.1'	36.3''	36	12.4	3.4
93 GHz	2.2'	2.2'	15.3''	8	2.0	0.6
145 GHz	1.4'	1.4'	10.0''	10	2.0	0.6
225 GHz	1.0'	1.0'	6.6''	22	6.9	1.9
280 GHz	0.9'	0.9'	5.4''	54	16.7	4.6

TABLE III. The detection SNR of the (reconstructed) velocity and galaxy-density cross-correlation  $P_{vg}(k)$ . Velocities are reconstructed from the KSZ tomography using LSST and MegaMapper surveys, together with CMB measurements from SO, CMB-S4 and CMB-HD.

KSZ SNR	$z = 1.9$	2.6	3.45	4.45
LSST Y10 + CMB-HD	1087	879	351	51
LSST Y10 + CMB-S4	186	126	48	7
LSST Y10 + CMB-SO	87	59	23	4
MegaMapper + CMB-HD	1629	1051	453	129
MegaMapper + CMB-S4	254	154	78	31

$\Delta x_{\text{re}}^{\text{He}}$  (or  $Y_p$ ) after marginalizing over all other parameters. We find LSST Y1 and SO can potentially detect helium reionization at  $\{2\sigma, 4\sigma, 7\sigma\}$  significance for models 2, 1 and 3, respectively. For LSST Y10 and CMB-S4, we find the detection SNR will be  $\{4\sigma, 8\sigma, 13\sigma\}$ . For the futuristic MegaMapper and CMB-HD, the detection SNR can reach  $\{39\sigma, 56\sigma, 87\sigma\}$ .

The sensitivities on the parameters describing the helium reionization—given our fiducial model labeled 1—are shown in Fig. 2. The blue (orange) contours correspond to combination of LSST and CMB-S4 (MegaMapper and CMB-HD). In both cases we assume no prior information on the optical-depth and galaxy biases.<sup>7</sup> The innermost lighter-coloured contours assume 0.005 prior on the  $Y_p$  parameter, which can be provided from helium emission line measurements [57] as well as potentially the CMB [40,50]. We find assuming priors on  $Y_p$  improves the measurement accuracy on the other helium reionization parameters, most notably for LSST and CMB-S4. We show our forecasted sensitivities ( $1\sigma$  errors) in a table in Fig. 2. We find the combination of LSST and CMB-S4 can measure the time of helium reionization at a precision that would allow distinguishing between models 1 and 3 and put potentially

<sup>7</sup>Note that better sensitivity on optical depth or the galaxy biases only marginally improves the sensitivity of these experiments to helium reionization parameters, since the degeneracy between them and the bias parameters at each redshift is broken by the distinct redshift dependence of the models we consider.



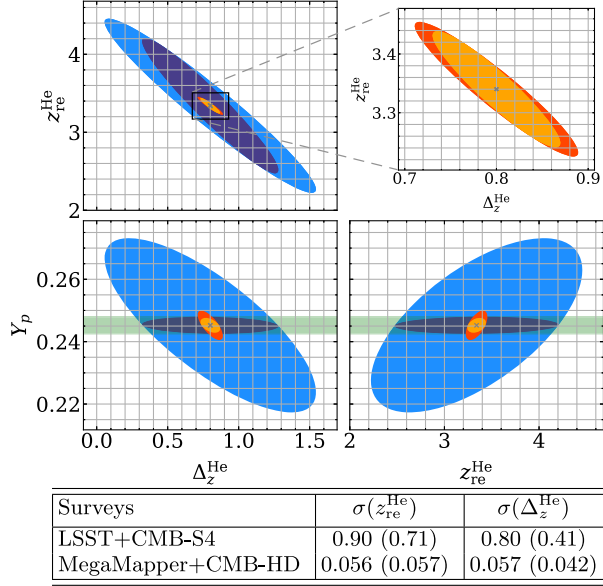


FIG. 2. The sensitivities ( $1\sigma$  errors) on the helium reionization parameters from two survey combinations: LSST and CMB-S4 shown with blue- and purple-colored contours, and MegaMapper and CMB-HD, shown with light- and dark-orange contours. The inner contours for each experiment correspond to assuming 0.005 prior on  $Y_p$ . The table shows the  $1\sigma$  errors on  $z_{\text{re}}^{\text{He}}$  and  $\Delta_z^{\text{He}}$ . The  $1\sigma$  errors on  $Y_p$  (without the  $Y_p$  prior) are 0.06 and 0.006, respectively. The bracketed sensitivities correspond to assuming 0.005 prior on the helium fraction  $Y_p$ .

informative lower limits on duration of helium reionization. With MegaMapper and CMB-HD, we find KSZ tomography can measure the redshift and the duration of reionization at much higher significance, potentially allowing distinguishing between similar models.

Interestingly, as demonstrated in Fig. 2, we find the combination of MegaMapper and CMB-HD may have a sensitivity to  $Y_p$  comparable to the accuracy of CMB and helium emission-line measurements. In order to assess further, we perform CMB forecasts on  $Y_p$  using FisherLens, a publicly available [58] forecasting software [59]. We take experimental specifications matching CMB-HD and with cosmological model parameters including the six standard  $\Lambda$ CDM parameters in addition to  $N_{\text{eff}}$ , and  $Y_p$ . We observe a CMB-HD-like experiment including both temperature and polarization information can be expected to achieve  $\sigma(Y_p) \simeq 0.004$  sensitivity and that adding  $\sigma(Y_p) \simeq 0.006$  measurement from KSZ tomography from helium reionization can improve the error on  $Y_p$  by  $\sim 15\%$ . We find that this improvement leads to a  $\sim 10\%$  reduction in  $N_{\text{eff}}$  error, due to the partial breaking of the degeneracy suffered between the two parameters, suggesting KSZ measurements of helium reionization can potentially improve our understanding of relativistic species.

We have omitted the potential effect of helium reionization on the selection function of high- $z$  quasars and galaxies. Across helium reionization, the ionizing processes can

modulate the ultraviolet background fluctuations, the star formation and the absorption lines used for inferring the redshift with spectroscopic imaging surveys such as DESI and MegaMapper. Such effects can potentially cause significant changes that need to be taken into account in the selection function of these surveys and likely need to be modeled for an unambiguous characterization of helium reionization, as well as using more accurate inputs (such as the galaxy bias and number density) when performing forecasts in the future.

Throughout this paper, we used the so-called “box” formalism introduced in Refs. [28–30]. The benefit of this formalism is its simplicity, while using redshift bins on the light cone is likely a more accurate representation of KSZ tomography in practice, as discussed in Refs. [28,56,60], for example.<sup>8</sup> Here, our goal was to produce easy-to-reproduce forecasts that access and highlight the prospects of detecting and characterizing helium reionization.

The epoch of helium reionization carries a large amount of information about astrophysics and cosmology that can potentially be accessed in the foreseeable future. As it occurs at lower redshifts, it allows the utilization of the significant statistical power afforded by the LSS and CMB cross-correlation program—a quality likely not shared with hydrogen reionization.

Reconstructing velocities at high SNR with future surveys will provide precise tests of fundamental physics. We have shown here that this also provides a new path to detecting and characterizing helium reionization. These measurements will not require new experiments other than those being built or proposed, offering new opportunities and avenues for exploration for both cosmology and astrophysics.

## ACKNOWLEDGMENTS

We thank Joel Meyers, Colin Hill, Alex van Engelen and Patrick Hall for useful discussions. This work was started in part at the Aspen Center for Physics, which is supported by National Science Foundation (NSF) Grant No. PHY-1607611. S. C. H. is supported by the Horizon Fellowship from Johns Hopkins University. S. C. H. also acknowledges the support of a grant from the Simons Foundation at the Aspen Center for Physics. S. F. is supported by the Physics Division of Lawrence Berkeley National Laboratory.

<sup>8</sup>In addition, formalizing KSZ tomography on the light cone has the benefit of better capturing the redshift dependence of the signal, particularly in the case of spectroscopic surveys where one can separate the redshift range in many bins, as well as better capturing the degrading effect of CMB foregrounds which may lead to biases or enhanced noise for the reconstruction, for example, which may be a limiting factor. Going forward, KSZ tomography will need testing against realistic simulations, including non-Gaussian and correlated foregrounds, and with accurate modeling of the baryon distribution.

G. P. H. is supported by Brand and Monica Fortner and the Canadian Institute for Advanced Research. M. C. J. is supported by the National Science and Engineering Research Council through a Discovery grant. This research was supported in part by Perimeter Institute for Theoretical Physics. Research at Perimeter Institute is supported by

the Government of Canada through the Department of Innovation, Science and Economic Development Canada and by the Province of Ontario through the Ministry of Research, Innovation and Science. M. K. was supported by NSF Grant No. 2112699 and the Simons Foundation. P. L. is supported by NSF Grant No. 2206602.

- 
- [1] N. P. Ross, I. D. McGreer, M. White, G. T. Richards, A. D. Myers, N. Palanque-Delabrouille, M. A. Strauss, S. F. Anderson, Y. Shen, W. N. Brandt, C. Yèche, M. E. C. Swanson *et al.*, *Astrophys. J.* **773**, 14 (2013).
  - [2] D. Masters, P. Capak, M. Salvato, F. Civano, B. Mobasher, B. Siana, G. Hasinger, C. D. Impey, T. Nagao, J. R. Trump, H. Ikeda, M. Elvis, and N. Scoville, *Astrophys. J.* **755**, 169 (2012).
  - [3] I. D. McGreer, L. Jiang, X. Fan, G. T. Richards, M. A. Strauss, N. P. Ross, M. White, Y. Shen, D. P. Schneider, A. D. Myers, W. N. Brandt, C. DeGraf, E. Glikman, J. Ge, and A. Streblyanska, *Astrophys. J.* **768**, 105 (2013).
  - [4] I. D. McGreer, X. Fan, L. Jiang, and Z. Cai, *Astron. J.* **155**, 131 (2018).
  - [5] Z. Pan, L. Jiang, X. Fan, J. Wu, and J. Yang, *Astrophys. J.* **928**, 172 (2022).
  - [6] Y. Shen and L. C. Ho, *Nature (London)* **513**, 210 (2014).
  - [7] P. F. Hopkins, A. Lidz, L. Hernquist, A. L. Coil, A. D. Myers, T. J. Cox, and D. N. Spergel, *Astrophys. J.* **662**, 110 (2007).
  - [8] T. M. Schmidt, G. Worseck, J. F. Hennawi, J. X. Prochaska, and N. H. M. Crighton, *Astrophys. J.* **847**, 81 (2017).
  - [9] K. Inayoshi, E. Visbal, and Z. Haiman, *Annu. Rev. Astron. Astrophys.* **58**, 27 (2020).
  - [10] G. T. Richards, M. A. Strauss, X. Fan, P. B. Hall, S. Jester, D. P. Schneider, D. E. Vanden Berk, C. Stoughton *et al.*, *Astron. J.* **131**, 2766 (2006).
  - [11] P. Jakobsen, A. Boksenberg, J. M. Deharveng, P. Greenfield, R. Jedrzejewski, and F. Paresce, *Nature (London)* **370**, 35 (1994).
  - [12] W. Zheng, A. Meiksin, K. Pifko, S. F. Anderson, C. J. Hogan, E. Tittley, G. A. Kriss, K. Chiu, D. P. Schneider, D. G. York, and D. H. Weinberg, *Astrophys. J.* **686**, 195 (2008).
  - [13] D. Syphers and J. M. Shull, *Astrophys. J.* **784**, 42 (2014).
  - [14] F. Calura, E. Tescari, V. D’Odorico, M. Viel, S. Cristiani, T. S. Kim, and J. S. Bolton, *Mon. Not. R. Astron. Soc.* **422**, 3019 (2012).
  - [15] M. Viel, G. D. Becker, J. S. Bolton, and M. G. Haehnelt, *Phys. Rev. D* **88**, 043502 (2013).
  - [16] E. Boera, M. T. Murphy, G. D. Becker, and J. S. Bolton, *Mon. Not. R. Astron. Soc.* **456**, L79 (2016).
  - [17] P. R. Upton Sanderbeck, A. D’Aloisio, and M. J. McQuinn, *Mon. Not. R. Astron. Soc.* **460**, 1885 (2016).
  - [18] P. La Plante, H. Trac, R. Croft, and R. Cen, *Astrophys. J.* **841**, 87 (2017).
  - [19] P. La Plante, H. Trac, R. Croft, and R. Cen, *Astrophys. J.* **868**, 106 (2018).
  - [20] J. S. Bolton, E. Puchwein, D. Sijacki, M. G. Haehnelt, T.-S. Kim, A. Meiksin, J. A. Regan, and M. Viel, *Mon. Not. R. Astron. Soc.* **464**, 897 (2017).
  - [21] D. Syphers, S. F. Anderson, W. Zheng, A. Meiksin, D. P. Schneider, and D. G. York, *Astron. J.* **143**, 100 (2012).
  - [22] G. D. Becker, J. S. Bolton, M. G. Haehnelt, and W. L. W. Sargent, *Mon. Not. R. Astron. Soc.* **410**, 1096 (2011).
  - [23] E. Boera, M. T. Murphy, G. D. Becker, and J. S. Bolton, *Mon. Not. R. Astron. Soc.* **441**, 1916 (2014).
  - [24] K. N. Telikova, P. S. Shternin, and S. A. Balashev, *Astrophys. J.* **887**, 205 (2019).
  - [25] E. V. Linder, *Phys. Rev. D* **101**, 103019 (2020).
  - [26] M. Bhattacharya, P. Kumar, and E. V. Linder, *Phys. Rev. D* **103**, 103526 (2021).
  - [27] R. A. Sunyaev and Y. B. Zeldovich, *Comments Astrophys. Space Phys.* **2**, 66 (1970).
  - [28] A.-S. Deutsch, E. Dimastrogiovanni, M. C. Johnson, M. Münchmeyer, and A. Terrana, *Phys. Rev. D* **98**, 123501 (2018).
  - [29] K. M. Smith, M. S. Madhavacheril, M. Münchmeyer, S. Ferraro, U. Giri, and M. C. Johnson, *arXiv:1810.13423*.
  - [30] M. Münchmeyer, M. S. Madhavacheril, S. Ferraro, M. C. Johnson, and K. M. Smith, *Phys. Rev. D* **100**, 083508 (2019).
  - [31] P. Zhang and M. C. Johnson, *J. Cosmol. Astropart. Phys.* **06** (2015) 046.
  - [32] S. C. Hotinli, J. B. Mertens, M. C. Johnson, and M. Kamionkowski, *Phys. Rev. D* **100**, 103528 (2019).
  - [33] J. I. Cayuso and M. C. Johnson, *Phys. Rev. D* **101**, 123508 (2020).
  - [34] M. A. Alvarez, S. Ferraro, J. C. Hill, R. Hložek, and M. Ikape, *Phys. Rev. D* **103**, 063518 (2021).
  - [35] S. Ferraro and K. M. Smith, *Phys. Rev. D* **98**, 123519 (2018).
  - [36] K. M. Smith and S. Ferraro, *Phys. Rev. Lett.* **119**, 021301 (2017).
  - [37] S. C. Hotinli and M. C. Johnson, *Phys. Rev. D* **105**, 063522 (2022).
  - [38] A. Aghamousa *et al.* (DESI Collaboration), *arXiv:1611.00036*.
  - [39] LSST Science Collaboration *et al.*, *arXiv:0912.0201*.
  - [40] K. N. Abazajian *et al.* (CMB-S4 Collaboration), *arXiv:1610.02743*.
  - [41] K. Abazajian *et al.*, *arXiv:1907.04473*.
  - [42] D. J. Schlegel *et al.*, *Bull. Am. Astron. Soc.* **51**, 229 (2019).

- [43] S. Ferraro, N. Sailer, A. Slosar, and M. White, [arXiv:2203.07506](#).
- [44] Y. Ali-Haïmoud and C. M. Hirata, *Phys. Rev. D* **83**, 043513 (2011).
- [45] P. La Plante, H. Trac, R. Croft, and R. Cen, *Astrophys. J.* **841**, 87 (2017).
- [46] E. Lusso, G. Worseck, J. F. Hennawi, J. X. Prochaska, C. Vignali, J. Stern, and J. M. O'Meara, *Mon. Not. R. Astron. Soc.* **449**, 4204 (2015).
- [47] M. White *et al.*, *Mon. Not. R. Astron. Soc.* **424**, 933 (2012).
- [48] F. Haardt and P. Madau, *Astrophys. J.* **746**, 125 (2012).
- [49] S. Aiola *et al.* (CMB-HD Collaboration), [arXiv:2203.05728](#).
- [50] N. Aghanim *et al.* (Planck Collaboration), *Astron. Astrophys.* **641**, A6 (2020); **652**, C4(E) (2021).
- [51] Y. Harikane, M. Ouchi *et al.*, *Publ. Astron. Soc. Jpn.* **70**, S11 (2018).
- [52] Y. Harikane *et al.*, *Publ. Astron. Soc. Jpn.* **70**, S11 (2018).
- [53] J. Aguirre *et al.* (Simons Observatory Collaboration), *J. Cosmol. Astropart. Phys.* **02** (2019) 056.
- [54] S. C. Hotinli, K. M. Smith, M. S. Madhavacheril, and M. Kamionkowski, *Phys. Rev. D* **104**, 083529 (2021).
- [55] A. Lewis, A. Challinor, and A. Lasenby, *Astrophys. J.* **538**, 473 (2000).
- [56] J. Cayuso, R. Bloch, S. C. Hotinli, M. C. Johnson, and F. McCarthy, *J. Cosmol. Astropart. Phys.* **02** (2023) 051.
- [57] E. Aver, K. A. Olive, and E. D. Skillman, *J. Cosmol. Astropart. Phys.* **07** (2015) 011.
- [58] <https://github.com/ctrendafilova/FisherLens>.
- [59] S. C. Hotinli, J. Meyers, C. Trendafilova, D. Green, and A. van Engelen, *J. Cosmol. Astropart. Phys.* **04** (2022) 020.
- [60] A.-S. Deutsch, M. C. Johnson, M. Münchmeyer, and A. Terrana, *J. Cosmol. Astropart. Phys.* **04** (2018) 034.